The Use of Multi-Modal Satellite Imagery for Detection of Palmyra Trees: A Machine Learning-Based Approach

Author

TAYYEBA JAVED

Regn Number 00000117376

Supervisor

DR. KHURRAM KAMAL

DEPARTMENT OF MECHATRONICS ENGINEERING

COLLEGE OF ELECTRICAL & MECHANICAL ENGINEERING

NATIONAL UNIVERSITY OF SCIENCES AND TECHNOLOGY

ISLAMABAD

FEBRURARY, 2018

The Use of Multi-Modal Satellite Imagery for Detection of Palmyra Trees: A Machine Learning-Based Approach

Author

TAYYEBA JAVED

Regn Number 00000117376

A thesis submitted in partial fulfillment of the requirements for the degree of

MS Mechatronics Engineering

Thesis Supervisor:

DR. KHURRAM KAMAL

Thesis Supervisor's Signature: _____

DEPARTMENT OF MECHATRONICS ENGINEERING

COLLEGE OF ELECTRICAL & MECHANICAL ENGINEERING

NATIONAL UNIVERSITY OF SCIENCES AND TECHNOLOGY,

ISLAMABAD

FEBRUARY, 2018

Declaration

I certify that this research work titled "*The Use of Multi-Modal Satellite Imagery for Detection of Palmyra Trees: A Machine Learning-Based Approach"* is my own work. The work has not been presented elsewhere for assessment. The material that has been used from other sources it has been properly acknowledged / referred.

Signature of Student

Tayyeba Javed

Language Correctness Certificate

This thesis has been read by an English expert and is free of typing, syntax, semantic, grammatical and spelling mistakes. Thesis is also according to the format given by the university.

Signature of Student

Tayyeba Javed

0000011776

Signature of Supervisor

Copyright Statement

- Copyright in text of this thesis rests with the student author. Copies (by any process) either in full, or of extracts, may be made only in accordance with instructions given by the author and lodged in the Library of NUST College of E&ME. Details may be obtained by the Librarian. This page must form part of any such copies made. Further copies (by any process) may not be made without the permission (in writing) of the author.
- The ownership of any intellectual property rights which may be described in this thesis is vested in NUST College of E&ME, subject to any prior agreement to the contrary, and may not be made available for use by third parties without the written permission of the College of E&ME, which will prescribe the terms and conditions of any such agreement.
- Further information on the conditions under which disclosures and exploitation may take place is available from the Library of NUST College of E&ME, Rawalpindi.

Acknowledgements

I am thankful to Allah Subhana-Watala for His countless blessings. I am grateful to my parents, for their support and trust in me. I am thankful towards my co-supervisor Dr. Senthan Mathavan's hard work and efforts with me. Lastly, I appreciate Dr. Khurram Kamal for his supervision and motivation throughout thesis.

Dedicated to my parents and siblings

Abstract

A manual census of trees over a large geographic area can be very costly. Remote sensing is a powerful tool for the task. In this regard, this research focuses on the Google Earth image-based detection and counting of Palmyra trees in the northern part of Sri Lanka. Freely accessible Google Earth images are for the first time used here for the detection of specific tree type. Color information is used to identify their foliage. As the color information itself can be ambiguous at times, a complimentary analysis in the form of the identification of shadows is also carried out. Here, the fact that these tall trees throw a considerable shadow on the ground or other lower lying features is exploited. Phase Stretch Transform is used to identify the shadows. Furthermore, object-based image analysis is used on high resolution QuickBird images for detection of Palmyra on larger area. Multi-resolution segmentation and supervised nearest neighbor classification is used for that purpose. The detection results in successfully extracted Palmyra among other vegetation in Google Earth images and shows with a precision of 92.6% and recall of 88%. On QuickBird images, precision and recall values are found to be 92% and 95.5% respectively.

Key Words: *Remote sensing, Palmyra tree detection, Phase Stretch Transform, Shadow detection*

Table of Contents

List of Figures

List of Tables

1.INTRODUCTION

Forest mapping has extensive variety of utilizations, fundamentally in mapping the density of forests and the rate of deforestation in a region. Customarily a tree registration is done physically or through remote detecting strategies, which are tedious and exorbitant. The goal of this research is to evaluate Google Imagery as a potential source for the detection of Palmyra trees. Furthermore, high resolution QuickBird images will be used for detection of Palmyra trees on a larger area.

Sri Lanka had over 10 million Palmyra trees three decades ago, concentrated in the Jaffna and Mannar regions [1] . The numbers reduced significantly in the past decade due to the expansion of urban areas during the civil war. The trees have been cut down at rapid pace to be used in housing and to provide land for urban population. Wood from the extensive cutting of Palmyra trees have been used for the fortification of bunkers and shelters against bombardment in the war. They are also being replaced by coconut fields, which are economically more advantageous. Getting a headcount of these trees and concretely establishing the descending trend in their number will create an awareness of the seriousness of the issue. An automated tree counting procedure will accomplish both these tasks in a straightforward manner.

Palmyra trees are also found in many other Indian Ocean countries in South and Southeast Asia. The tree has a lifespan of more than 100 years. It usually grows to a height of 30 m standing tall above the foliage of other types of trees, and the trunk may have a circumference of over 1.5 meters at the base. The black colored trunk is cylindrical in shape. In addition, its green-bluish leaves are in the shape of fronds growing up to 3 m in length. With 10-20 individual fronds coming out at the top end of a tree, its foliage resembles a sphere in its totality and is a distinct feature on the skyline of the region.

Their uses range from household items to construction material, source of sugar toddy to timber. Sap is used as sweet candy, toddy and vinegar. Versatile products are obtained from leaves e.g. hatching of roofs and screening as fence, handicrafts like baskets, mats, hats etc. Its

string wood is used in construction, in making boats, furniture and as fuel. Medicinal products are obtained from its pulp; fibre is used in making brushes.

Figure 1.1. A Palmyra tree

Google Earth imagery is free of cost and available in high resolution, having been gathered via different sources. Other high spatial resolution satellite imagery is not readily available for the public. It is also cloud and snow free. In this research, the unique characteristics of the leaf structure of Palmyra, as seen from above, is exploited towards its automated detection. In this regard, this is the first effort, where Google Earth imagery is used to detect a specific type of tree. Different vision-based techniques are used here for Palmyra trees detection using their distinctive features.

QuickBird images are multispectral and a higher spatial resolution of 60 cm. In this research, spatial, spectral and textural properties of Palmyra trees are used for their detection. The density mapping of Palmyra trees will be done from coloured images of QuickBird satellite.

The thesis is organized in following sections. Chapter 2 presents the previous work related to remote sensing techniques used in forestry, background tree detection algorithms. Chapter 3

explains the theory behind the chosen methods while in chapter 4 algorithm is explained. The results and discussion are presented in chapter 5. Chapter 6 discusses the conclusions, novelty of research and future work.

2.LITERATURE REVIEW

This chapter presents literature review regarding various applications of remote sensing in the field of forest mapping. Different modes of remote sensing are also compared here. Then a detailed background knowledge is provided on the detection of trees, various methods have been categorized and discussed.

2.1. Application of remote sensing in forestry

Remote sensing has wide range of applications in forestry, out of which few are described in detail here. It is used for the mapping of forest area, change detection occurred in an area, and for modelling of resource management.

2.1.1. Mapping/statistics generation of forest cover

Forestry mapping includes determination of the forest type, density estimation and the evaluation of bio-diversity. The measurement of tree parameters such as height and diameter of trunk, the volume, circumference, shape of canopy. Lennartz et al. [2] mapped forest tree types in northeastern United States.

2.1.2. Change detection

'Change detection' is found in time lapse images to estimate how much change occurred in objects of interest in certain time span. One of its main uses is to estimate rate of deforestation. Margono et al. [3] mapped deforestation in Indonesia over 20 years using Landsat images. Qamer et al. [4] estimated forest degradation over a period of 20 years in Himalayan mountain forests. Likewise, those areas, where there was no previous tree cover can also be identified. With the help of the images of before and after a wildfire, the fire damage can be estimated [5]

2.1.3. Modelling of resource management

Remote sensing techniques can also help in management of resources e.g. estimation of timber volume and biomass and finding suitable habitat for certain species of interest.

Furthermore, forest fire risk zones can also be mapped so that frequency of possible fires can be minimized [6] Dong et al. [7] used Principal Component Analysis (PCA) to find the relationship between forest fire potentials and environmental factors. Then a fuel-based, a topography-based, and an anthropogenic-factor fire risk maps are formed in Geographic Information System (GIS). The final fire risk map was generated from these three maps.

2.2. Remote sensing data

Data Acquired from Remote sensing techniques can be categorized as airborne or spaceborne, depending on the module on which imaging device is attached. It affects the area of coverage and resolution of the data.

2.2.1. Airborne Imagery

In airborne remote sensing, the imager is mounted on an aircraft that flies over the site area. The images obtained from the camera are high resolution images usually less than 40 cm/pixel. On the downside, this push-broom method gives a low area coverage and high cost, compared to space borne imagery.

Light detection and Ranging (LiDAR) is a remote sensing technique used to measure ranges and distances to the Earth by using pulsed laser for target illumination. A LiDAR unit consists of a laser scanner, a GPS receiver for the measurement of the 3D position of the tracked system (e.g. aircraft, drone), and an Inertial Measurement Unit (IMU) to track airplane orientation, i.e. roll, pitch, and yaw. Vegetation at species level can be mapped with relatively high accuracy using LiDAR.

Airborne Visible Infrared Imaging Spectrometer (AVIRIS) has the capability to acquire images with 224 spectral bands from visible and near infrared to short wave infrared. It provides spatial resolution from meters to dozens of meters. The jerking of airplane needs to be incorporated, fine spectral resolution makes spectral signature within an object vary that makes detection challenging. Vegetation at community level or species level can be mapped using AVIRIS.

2.2.2. Spaceborne Imagery

In spaceborne remote sensing, a sensor is mounted on a satellite to cover a large area. Its spatial resolution can vary from centimeters to thousands of meters. Satellite sensors have the following parameters.

2.2.2.1. Spatial Resolution

The spatial resolution specifies the region on the ground covered by a pixel in the image. Two nearby objects would be differentiable if the resolution is high. Based on the spatial resolution of the sensor, vegetation can be mapped at different scales. Coarse resolution images can help in finding overall vegetation area in the scene, but from high resolution images different species of the trees can be identified.

Table 2-1: Spatial resolution and vegetation mapping scale

Spatial Resolution (m)	**Vegetation mapping**
<1	
1	Mapping at local to regional scale with identifiable species
2.5	Maps vegetation at regional scale, tree communities or species can be identified
15	Maps vegetation at regional scale, main tree species can be recognized
30	Maps vegetation at regional scale
90	Maps tree groves at state level
250 - 1000	Maps vegetation over globe, continents or states

2.2.2.2. Spectral Resolution

The capacity of a sensor to characterize fine wavelengths is known as spectral resolution of that sensor. A finer division of electromagnetic spectrum yields narrower wavelength ranges for a particular channel.

Panchromatic is a single channel black and white image. Whereas, a multispectral image contains 4 to 5 bands of different wavelengths. Super-spectral image contains tens of bands with different wavelengths. On the other hand, hyperspectral image contains hundreds of bands with almost continuous wavelength variation.

2.2.2.3. Temporal Resolution

Amount of time needed for a satellite to revisit and acquire data from exactly the same point on Earth is defined as the temporal resolution. Landsat has a temporal resolution of 16 days, whereas the revisit rate of IKONOS is 3–5 days.

2.3.Common Satellite Sensors

The multispectral or hyperspectral imager is attached to sun synchronous satellites, which orbit at several hundred kilometers from the Earth. Their spatial resolutions are in meters/pixel. Some common satellite sensors are:

1. LANDSAT TM: It has medium to rough spatial resolution with multispectral data, spatial resolution is 30 m/pixel. Landsat 4 and 5 have 7 spectral bands, while Landsat 8 has 11 bands.
2. LANDSAT ETM+: It provides intermediate to rough resolution images. Panchromatic images have resolution of 15 m while multispectral bands are two times lower in resolution. Each image tile covers 185 sq. km area.
3. MODIS: This satellite provides a very low spatial resolution of 250-1000 m/pixel and provides super-spectral data i.e. 36 bands.
4. Hyperion: It provides hyperspectral images with 220 bands, whose spectral values range from visible to short wave infrared (SWIR) and has a spatial resolution of 30 m.
5. SPOT: It provides medium spatial resolutions that range from 20 m to 2.5 m. It has 5 spectral bands. Revisit cycle is 26 days.

6. QuickBird: It provides high spatial resolution image with panchromatic and multispectral data. The resolution is 0.6 m/pixel. Each image tile covers 16.5 sq. km area. Revisit cycle is 1–3.5 days.
7. IKONOS: It provides fine resolution imagery with multispectral data. It has four spectral bands and a panchromatic with resolution 4 m and 1 m respectively. The single scene is 11 x 11 sq. km.
8. WorldView: WorldView-2 collects 8 band multispectral data of 1.84 m resolution. The panchromatic band has 0.46 m resolution. While in WorldView-3 satellite multispectral bands have 1.24 m resolution and panchromatic has 0.31 m resolution.
9. Orbview: It provides panchromatic image of 1 m resolution and multispectral bands with four times less resolution. Spectral range is 450-900 nm. It has 5 spectral bands.

2.4.Vegetation spectral signature

Features on the Earth reflect, absorb, transmit, and emit electromagnetic energy from the sun. Sun's energy that reflects from any material creates a unique fingerprint that is defined as the spectral signature of that particular material. Plants are highly reflective in near infrared. They have low reflectance in the visible region, so this unique combination for most vegetation types is known as the vegetation spectral signature.

Chlorophyll absorbs energy at about 0.45 μm (blue) and 0.67 μm (red) wavelength. A healthy vegetation is perceived as green in color due to its reflectance of green light. Stressed plants, due to disease or insect attacks, tend to appear yellow due to less absorption of chlorophyll in blue and red bands. Table given below shows the reflectance of vegetation in different wavelength bands.

Table 2-2: Reflectance of vegetation in different wavelength bands

Wavelength (μm)	Reflectance of vegetation
0.53 - 0.59	Green reflectance for vegetation discrimination
0.58 - 0.62	Yellow tree crown due to insect disease
0.63 - 0.69	Chlorophyll absorption

0.76 - 0.90	To classify healthy vegetation
1.55 - 1.75	Sensitivity to amount of water in plants

2.4.1. Vegetation Indices

A Vegetation Index (VI), is mathematical grouping or spectral transformation of two or more bands designed to enhance the spectral properties of green plants so that they appear different from other image objects. It is used to distinguish between soil and vegetation, or to indicate the percentage cover of vegetation. Simple Ratio (SR) and Normalized Difference Vegetation Index (NDVI) are common vegetation indices.

2.5. Background knowledge

2.5.1. Google Earth Imagery based detections

Google Earth provides high resolution imagery with no clouds and snow, little haze and fewer shadows. Google acquire images from different sources, e.g. commercial satellite companies like DigitalGlobe or aerial photographs from airplanes, drones, etc. The age of imagery for high resolution varies between 6 months and 5 years.

Researchers have used Google Earth images in various applications. Mering et al. [8] extracted urban areas from Google Earth images using image processing techniques. Guo et al. [9] removed shadows of tall buildings in Google Earth images, Cha et al. [10] and Kaimaris et al. [11] used Google Earth for validation of detection results.

Taylor et al. [12] mapped agriculture sites and classified park areas, schools, residences, and community gardens using Google Earth in conjunction with ArcMap for the city of Chicago. Ploton et al. [13] applied texture analysis on Google Earth images for the detection of tropical forests to estimate biomass.

Nowak et al. [14] used Google Earth imagery to detect trees and invulnerable cover change for 20 US cities. Hu et al. [15] used object-based classification on Google Earth images for land use and cover mapping. They performed multi-scale image segmentation, to create image objects, on eCognition software. Afterwards, they selected eight most relevant object features and classified using rule sets. They validated results from QuickBird images of the same area, and have shown that Google Earth has potential to be used in land cover mapping. Tree detection from Google Earth images has never done before.

2.5.2. Palm tree detections

Gougeon et al. [16] used high spatial resolution images and a valley following technique i.e. presence of shades between crowns and rule-based crown delineation to get single tree crowns. They applied lower threshold to remove the small area of shade, and to find local minima which are deepest shades, from these points (8-connected pixels) followed valley of shades which separates tree crowns.

Shafri et al. [17] used Grey Level Co-occurrence Matrix (GLCM) for texture analysis of oil palm trees. Sobel edge filter is used to detect edges of trees, and then by thresholding oil palm trees are retrieved. But the extracted oil palm trees are irregular in shape, so they were refined by morphology reconstruction. Oil palm trees are counted based on the blob analysis. The disadvantage of the proposed approach is that it only uses the hyperspectral images.

Gebreslasie et al. [18] detected local peak to locate individual trees in Eucalyptus plantation forests. To suppress noise, they used a Gaussian filter for image smoothing. They employed the semi-variogram to determine the size of the window for local peak detection. Srestasathiern et al. [19] applied non-maximal suppression to differentiate between oil palm and non-oil palm samples using local peak detection on vegetation index image.

Alessio et al. [20] used a shadow detection technique to detect palms. They applied mean, standard deviation filters and mathematical morphology to get high contrast shadowy areas, and later classified the shadows as palm and non-palm.

2.5.3. Image Processing techniques

Basic characteristics of remotely sensed images are their color, texture, shape, size, shadow, pattern etc. The researchers have used different image processing techniques and algorithms to extract trees based on these characteristics.

Puissant et al. [21] used GLCM in texture analysis of panchromatic image of high resolution SPOT imagery. This second order statistical approach describes the grey value relationships in the neighborhood of the current pixel. Homogeneity, dissimilarity, entropy, angular second moment were the four features used. The output image and multispectral images are then classified using discriminant analysis. Pacifici et al. [22] used six GLCM features and two first order features i.e. mean and variance for feature extraction of land cover types in urban areas.

Culvenor [23] proposed an approach for automatically demarcating tree crowns on the imagery of native Eucalypt forests in Australia. The methodical sequence first detects the centroid of tree crown because by detecting local radiometric maxima yields the image coordinates of the possible crown peak. The construction of boundaries between all likely tree crowns is done using the local maximum pixels. The computation of threshold for combining connecting pixels within the same boundary defined by local maxima pixels into a unique crown is done using the digital number/brightness of the obtained maxima pixel.

2.5.4. Image Segmentation

In image analysis, different techniques for image segmentation are used. The goal is to divide image into segments so that it extracts all objects of interest. Global thresholding is one of the simplest image segmentation method that has results that are normally low in quality.

Region growing algorithms are grouping pixels from some initial seed points. Efficiency of these algorithms depend upon seed points and they do not have criteria for stopping of clustering of pixels. Yang et al. [24] used multi-band watershed segmentation for crown

demarcation of deciduous trees, whose boundaries are not much distinct compared to coniferous. They showed that its results are better compared to valley-following techniques.

Different algorithms of texture segmentation are used in many operational applications. From textures image, different characteristic features are obtained using spatial frequencies [25] , Markov Random Field (MRF) models [26] , co-occurrence matrices [28] , and wavelet coefficients [29] . Then these features are clustered into homogenous segments using clustering cost functions. These techniques are just applicable to images with the texture, not every data type.

Other segmentation techniques which consider spectral (color), textural properties and object size are multiresolution segmentation, quad-tree segmentation, and chessboard segmentation. The contrast split algorithm divides images as bright and dark objects. Bunting et al. [30] used chessboard segmentation in their algorithm for tree crown delineation in mixed species forests in Australia.

2.5.5. Image Analysis/ Classification

For low spatial resolution images, where pixel size is much larger than the object under consideration, then a sub-pixel analysis is used e.g. fuzzy classification and spectral mixture analysis techniques. Per-pixel techniques are used for medium resolution images, when pixel and object size is almost same. Whereas for high resolution images, when an object is divided in several pixels, object-based classification techniques are used. Image object can then be classified based on texture, context and geometry.

- Pixel-based
    - Supervised
    - Unsupervised
- Object-based

2.5.6. Supervised Classification

Supervised classification is used where classes are pre-defined and network is trained with known samples of classes. Classification accuracy of the supervised classification is heavily dependent on training data. If data does not do justice to representative of classes then classification will not be distinct. If class features are not unique then it can result in misclassification. Supervised classification may give results better than un-supervised, but it is time consuming.

2.5.6.1. Artificial neural network

Kavzoglu et al. [31] showed efficient design for Back-Propagation Neural Network (BP-NN) for classification of land cover types. Different design parameters of ANN like number of layers of neuron, number of hidden neurons, momentum factor, number of iterations, number of training samples were compared and an optimum design with highest accuracy was identified.

2.5.6.2. Random Forests

Jiang et al. [32] used images from different sensors to map aquatic vegetation (floating and submerged) using classification trees. Gislason et al. [33] used Random forests as classification technique for ten land cover types. Random forests work with large collection of decision trees or classification or regression trees CART, and can classify high dimensional data. Puissant et al. [34] classified wooden and non-wooden objects using Random Forest classifiers. Lee et al. [35] compared three algorithms, i.e. Classification and regression Trees (CART), Random Forest Trees (RFT), and Minimum Distance (MD) on basis of accuracy and kappa coefficient for detection of oil palm trees. They successfully detected palms in real-time with CART and RFT using all spectral bands.

2.5.6.3. Maximum Likelihood Classifier (MLC)

Walter 2004, performed Supervised Maximum Likelihood Classification to classify image objects. Shalaby et al. [36] used maximum likelihood classification for land cover mapping.

They detected land cover change between year 1987 to 2001 using LANDSAT images. The maximum likelihood classifier is based on statistical parameters, i.e. to classify an unknown pixel it evaluates variance and covariance of spectral response patterns of category.

Garrity et al. [37] co-registered two QuickBird images and a WorldView-2 image taken at different times to detect mortality of various tree species over the years. They classified live and dead trees using Gaussian Mixture Model GMM (Expectation Minimization algorithm). Dead trees were clearly distinguishable from live trees based on their higher reflectance in the visible bands, lower reflectance in the NIR band, lower NDVI values, and higher RGI values than live trees.

2.5.6.4. Genetic Algorithm

Tseng et al., [38] used genetic algorithm that is a 'stochastic search method', for classification of six land cover types in LANDSAT and AVIRIS images. In genetic algorithm, parameters are encoded into strings of characters and fitness is evaluated, then chromosomes (string) crossover to get best child population, after that mutation occurs with some low probability, new population is evaluated again until convergence.

2.5.6.5. Support Vector Machines:

SVM being a supervised learning algorithm make use of class labelled training examples. SVMs are constructed by locating a set of hyper planes that separate two or more classes of data. SVM make use of these hyper planes to discover boundaries between the input classes. Support vectors are those elements of input data that defines the boundaries. SVM is a set of algorithms that finds maximum-margin hyperplanes in some space. By making use of training examples of labeled classes, SVM splits those classes by maximum-margin hyperplanes. SVM are capable of classifying overlapping and non-separable data. SVM make use of kernel functions instead of linear functions to deal with complex and non-separable data. Kernel functions enables SVM to classify data separated by non-linear boundaries. Kernel functions causes the linear algorithm to work in non-linear feature space. Radial basis function is used as a kernel in SVM to produce an infinite dimension feature space known as Hilbert Space.

Kernel functions are an alternative way of projecting the data into high dimensionality feature space to increase the computational power of the linear support vector machines. SVM-based classification can balance between accuracy attained on a given finite amount of training patterns and the ability to generalize to unknown data. Lardeux et al. [39] used SVMs to classify dense tropical vegetation with SAR data. SVMs outperformed Wishart classification approach. Dalponte et al. [40] used SVMs and data fusion of hyperspectral and LiDAR data for forest species classification. SVMs performed better than Gaussian maximum likelihood classification and k-NN technique.

2.5.7. Unsupervised Classification

In unsupervised classification, the network trains itself and stops when dataset forms distinct classes. Unsupervised classification is not time consuming and no prior knowledge of class features is needed.

2.5.7.1.K-means and Iterative Self-Organizing Data Analysis clustering

K-mean and the ISODATA clustering algorithms are unsupervised methods commonly used. Class label are not pre-defined, after training clusters are formed with minimum in-class variance. At first arbitrary cluster vector is assigned, then it classifies each pixel to the closest cluster based on Euclidean distance and then, the new cluster mean vectors are calculated based on all the pixels in one cluster. These steps are repeated until the gap between the iteration is smaller than certain threshold [42] Morsdorf et al. [43] used k-means clustering to segment single trees from lidar data. Blanzieri et al. [44] used nearest neighbor for classification of remotely sensed images.

2.5.7.2. Self-Organizing Maps

Gonçalves et al. [45] used self-organizing maps and agglomerative hierarchical methods for classification of land cover. The SOM is an unsupervised competitive learning. The SOM is used to map the original patterns of the image to a two-dimensional neural grid to form input feature map. Inactive prototypes are filtered out and clustering is done using an agglomerative hierarchical clustering method neural grid, it generates a dendrogram of clustered neurons with

different degrees of similarity. Then clustered are evaluated and labelled as water, vegetation, soil or urban areas.

Other unsupervised techniques used for classification are Fuzzy C-Means Clustering Algorithm and Fuzzy Maximum Likelihood Classification.

2.5.8. Object based Classification

Yu et al. [46] created image objects using Fractal Net Evolution Approach (FNEA) and it overcame the problem of salt-and-pepper effects from traditional per pixel classification approaches such as iterative self-organizing maps. Then classified different vegetation image objects using Maximum Likelihood Classifier. Xie et al. [47] used an object based geographic image retrieval approach for detecting Australian Pine. Irregular shaped image objects are formed by hierarchical multi-resolution segmentation that produces homogenous image objects by grouping pixels.

Ardila et al. [48] proposed object-based algorithm to identify tree crowns. It includes methods such as segmentation at multiple scales, local contrast segmentation, tree shadow analysis, local maxima filtering, morphological object reshaping and region growing. The classes are defined using spectral (color) and geometric features of objects. Grasslands are masked using segmentation at multiple scales and NIR segment homogeneity, tree crowns are detected using NDVI value which are greater than threshold, individual trees with high background contrast detected with geometric and spectral attributes. Small trees detected with shadow (sun illumination, spectral, geometric attributes) and local maxima filtering of NIR (local peak at tree crown), interlocked trees detected with morphological watershed segmentation, trees with low background contrast detected with local maxima filtering NIR and region based growing on gradient descent NIR, NDVI.

Tehrany et al. [49] showed object-based K nearest neighbor (KNN) performed better than pixel-based Decision Trees. Candare et al. [50] developed image objects of crops in LiDAR

data using rule sets in eCognition and performed classification using support vector machine (SVM).

Mallinis et al. [51] used multiresolution segmentation and nearest neighbor for forest vegetation mapping. They showed classification tree worked better than nearest neighbor classifier used object based classification for forest mapping. Image objects are formed using image segmentation, Object features are selected using Genetic Algorithm and then classes are assigned using Neural Networks.

2.6. Thesis aims and objectives

The scope of the research is quite broad, however, according to level of research and based on the literature review, the thesis aims and objectives can be defined as follows

- To devise an image processing technique to describe different Palmyra tree foliage characteristics such as shape, color, spectral signatures, and shading using QuickBird data and Google Earth data.
- To establish a detector to differentiate Palmyra trees from rest of background area using machine learning approach.
- To develop a user-friendly interface to demonstrate application of proposed technique.

3.METHODOLOGY

3.1. Study Area

Study area is northern part of Jaffna. Palmyra trees are found in South Asia mainly in Sri Lanka, Cambodia, and India are source of great revenue. The northern part of Sri Lanka is a dry zone, where the vegetation is not very dense. In the major part of this region, being a peninsula with criss-crossing coastal lagoons, the water and soil do not lend them to the easy growth of the flora that is found in the rest of the country. However, Palmyra trees are, or used to be, in abundance in this area. These trees are also found in many other Indian Ocean countries in South and Southeast Asia. The tree has a lifespan of more than 100 years. It usually grows to a height of 30 m standing tall above the foliage of other types of trees. In addition, its green-bluish leaves are in the shape of fronds growing up to 3 m in length. With 10-20 individual fronds coming out at the top end of a tree, its foliage resembles a sphere in its totality and is a distinct feature on the skyline of the region.

3.2.Dataset 1

Google Earth images are of latitude and longitude 9º49’31’’ and 80º08’58’’. Imagery date is March 19, 2016. This particular area is selected due to the good contrast of Google Earth

Figure 3.1. Original Google Earth Image

images. Vegetation area here includes Palmyra, paddy fields, coconut and other trees. Only coconut trees grow tall, but even they not to the heights of Palmyra trees. In this area colour and shadow of Palmyra leaves are differentiable among other vegetation, as seen in Figure 3.1. Palmyra trees have a unique pale green colour with a near spherical crown and this is proposed to be one of the detection criteria. Although their leaves exhibit a pale green color, the color separation is always not very distinct, especially at the edges. This is truly an issue for detection of Palmyra that are among paddy fields.

3.2.1. Algorithm for Palmyra detection in Google Earth images

To detect Palmyra trees in Google Earth images, hysteresis thresholding is applied to detect the foliage of Palmyra trees. The tall trees throw shades on the ground and these appear as dark areas. The acquisition time of images is early morning, so the direction of shadows with respect to foliage is west or south-west. Edges of the trees are detected using Phase Stretch Transform (PST) because common edge detectors like Sobel and Canny and 2nd order based edge detectors, like Cumani, gave rise to lots of false positives, e.g. edges of roads, houses and other trees.

In a combined foliage and edges images, only the foliage that is next to an edge is retained. For that reason, a trapezoid mask is applied to remove false positives. Flowchart of the algorithm is shown in Fig. 3.2. For the object detection problem, common performance metrics used to evaluate the quality of the algorithm are the precision and recall [53] The number of true positives (TP), false positives (FP), and false negatives (FN) are considered. A TP, here, is Palmyra tree that is correctly detected by the algorithm. A FN is Palmyra tree that is not detected by the method and FP represent objects that are identified as Palmyra tree but actually they are not. The precision and recall are given by:

$$precision = \frac{TP}{TP+FP} \quad (1)$$

$$recall = \frac{TP}{TP+FN} \quad (2)$$

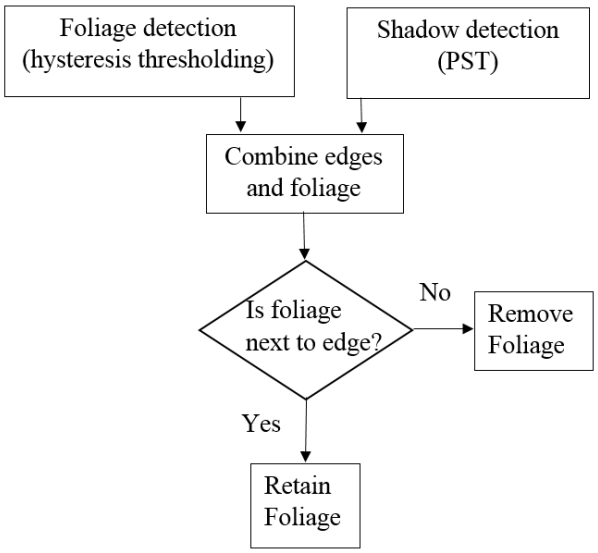

Figure 3.2. Algorithm Flowchart for Google Earth Images

3.3. Dataset 2

DigitalGlobe's QuickBird satellite provides the largest swath width, and high resolution imagery. The QuickBird satellite is capable of acquiring over 75 million square kilometers of imagery data annually. It is a sun-synchronous satellite with orbit inclination of 97.2 degree and orbit altitude of 450 km. QuickBird acquisition time for required area in Northern Sri Lanka is 2007-03-27 at 05:28:23. As images are acquired early morning, there are smaller shadows of Palmyra trees. Latitude and longitude of the area are from 9º49'26''N, 80º08'65'' E to 9º34'53'' N and 80º18'23'' E. This total area is covered in six images as shown in figure 3.3. where each image comprises of 100 km^2 area. Spatial resolution of panchromatic is 0.61 m and multispectral is 2.44 m while spectral resolution of the bands is:

- Panchromatic: 450 - 900 nm
- Blue: 450 - 520 nm
- Green: 520 - 600 nm
- Red: 630 - 690 nm

- Near InfraRed: 760 – 900nm

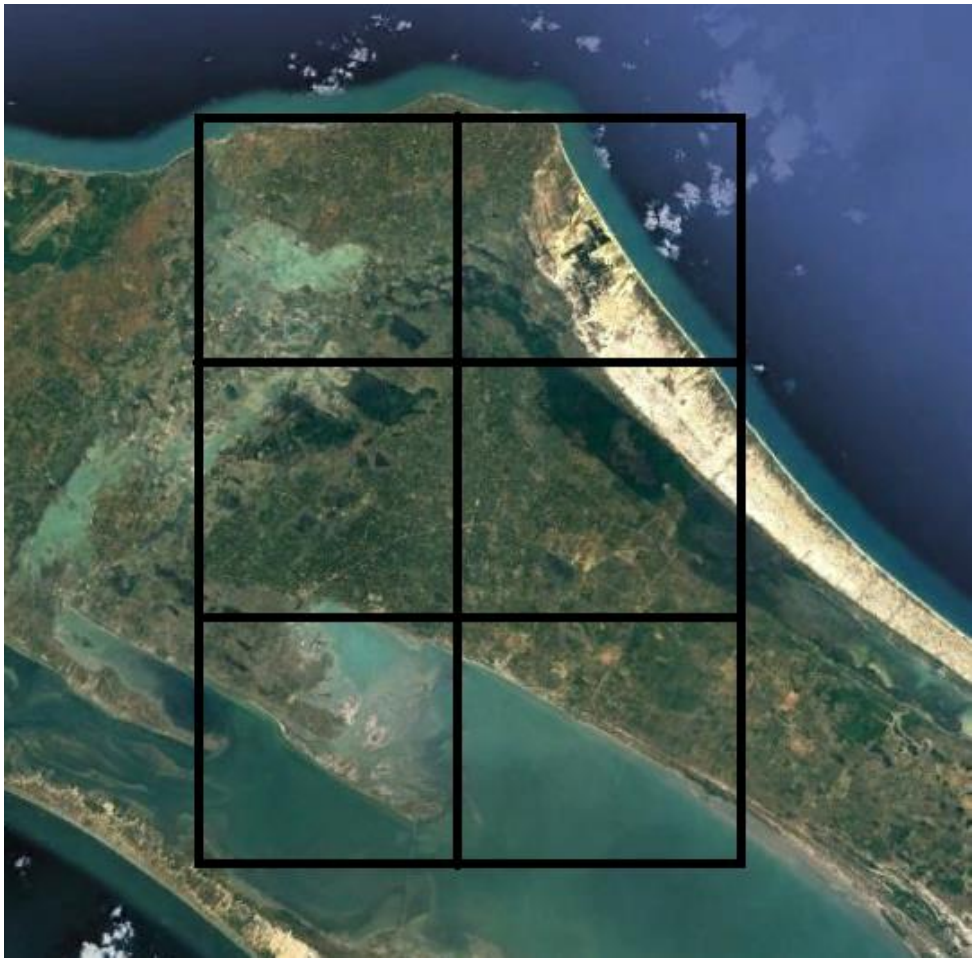

Figure 3.3. Area covered by QuickBird Images

3.3.1. Algorithm for Palmyra detection in QuickBird images

First QuickBird images are pan-sharpened using the Gram-Schmidt method. Then for object based image analysis, multi-resolution segmentation is applied on high resolution multispectral images. Resultant segmented image contains differentiable objects of Palmyra foliage. For supervised classification of Palmyra trees, nearest neighbor algorithm is trained with four object features whose values are in unique range for Palmyra tree foliage. Not only mean layer values are exploited, but texture analysis is also carried out. Algorithm flowchart is shown in figure 3.4.

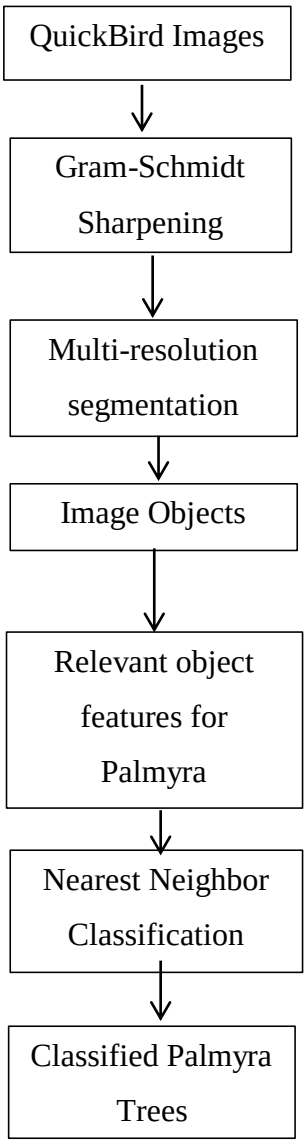

Figure 3.4. Algorithm Flowchart for QuickBird Images

4.TOOLS AND TECHNIQUES

4.1.Techniques used in Google Earth Images

4.1.1. Hysteresis thresholding

A hysteresis thresholding is usually used for edge detection using two thresholds. Pixel values above the high threshold are retained (white) and below the low threshold are removed (black). But pixels having intensities between the two threshold values will be retained only if they have a spatial connectivity to a pixel that has higher intensity than the upper threshold.

Here, segmentation of shades of a green color channel is done using band-based hysteresis thresholding. It uses four thresholds i.e., loose low, high thresholds and confident low, high threshold values. Loose thresholds are chosen as mean ± 0.95 times the standard deviation value of pixel intensities of pale green color of Palmyra, while confident thresholds are chosen as mean ± 0.7 times the standard deviation value of pixel intensities of pale green color. As Google Earth image is a 3-channel RGB image, hence this thresholding is applied to each channel data to extract Palmyra trees based on color. This yield to over-detection, where vegetation areas that have the same pale green color of Palmyra are also detected. But another differentiating characteristic of Palmyra trees is their shadow due to their long height.

4.1.2. Phase Stretch Transform (PST)

Asghari and Jalali [54] proposed an algorithm that uses the propagation of waves through a diffractive medium for the detection of edges. Gaussian localization kernel is used to smooth out the original image. On smoothed image, Phase Stretch Transform (PST) is applied i.e. a 2D phase function in the frequency domain, described as follows:

$$O[x,y] = \measuredangle\left[ifft2\left\{\tilde{\mathcal{K}}[p,q].\tilde{\mathcal{L}}[p,q].fft2\{I[x,y]\}\right\}\right] \quad (3)$$

The input image is represented by $I[x,y]$ where x and y are spatial variables, $O[x,y]$ is output phase image, $\measuredangle[\cdot]$ is the angle operator, *fft2* is the 2D Fast Fourier Transform, *ifft2* is the 2D Inverse Fast Fourier Transform, and p and q are one dimensional frequency variables. The

function $\tilde{\mathcal{L}}[p,q]$ is the frequency response of the localization kernel and the warped phase kernel $\widetilde{\mathcal{K}}[p,q]$ is described by a nonlinear frequency dependent phase:

$$\widetilde{\mathcal{K}}[p,q] = e^{j.\varphi[p,q]} \tag{4}$$

Arbitrary phase kernels can be used but here the following PST kernel phase is applied for which phase derivative is linear and can be represented with least the number of parameters:

$$\varphi[p,q] = S.\frac{W.f.tan^{-1}(W.f)-(1/2).ln(1+(W.f)^2)}{W.f_{max}.tan^{-1}(W.f_{max})-(1/2).ln(1+(W.f_{max})^2)} \tag{5}$$

Where $f = \sqrt{p^2+q^2}$, $tan^{-1}(\cdot)$ is the inverse tangent function, $ln(\cdot)$ is the natural logarithm, and f_{max} is the maximum frequency f. S and W are real-valued numbers related to the strength ($\mathcal{S}$) and warp ($\mathcal{W}$) of the phase profile applied to the image.

The amount of phase is frequency dependent because edges in image contain higher frequency features. Higher frequency features are detected with higher amount of phase. Parameters of the phase kernel that control edge detection process are phase strength, phase warp. Larger

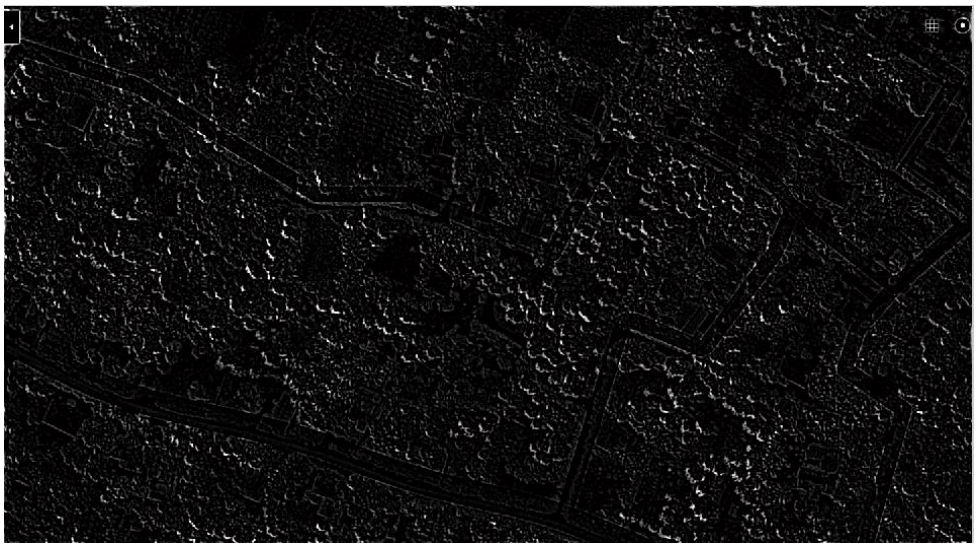

Figure 4.1. PST phase output

phase results in low noise in edge detection but with reduced spatial resolution. A larger phase

warp results in a sharper edge with increased noise. Entire tree shadow is extracted by binary thresholding of the PST output phase image. Figure 4.1 shows features detected using PST, when design parameters used for detection of Palmyra edges are S = 0.5, W= 12, localization kernel bandwidth Δf = 0.2.

4.1.3. Blob Analysis

As mentioned above, Palmyra trees have shadows to the east and southeast direction. The shadows of Palmyra are prominent due to their long height. Those vegetation areas which do not have edges to their left are not Palmyra trees. To remove false detections of trees, a trapezoid shaped mask is generated with respect to the centroid of edge of the tree. Only those tree blobs have retained that overlap or lie within trapezoid mask, as shown in Fig.4.2 (a). Tree blobs that do not have a tree shadow to their left indicate that they are not Palmyra trees, hence they are removed. There are few cases of lone trees where edge detection shows the shadow (i.e. presence of Palmyra) but tree blob was not detected in hysteresis thresholding (Fig. 4.2 b). Hence edges alone can be used for detection and counting of lone trees.

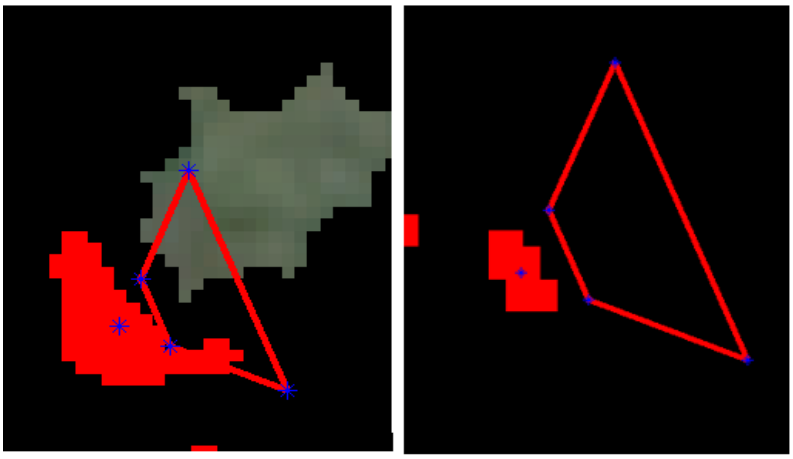

(a) (b)

Figure 4.2. (a) Trapezoid mask over foliage. (b) No foliage next to edge

4.1.4. Texture Analysis

Another problem faced during detection of Palmyra is presence of paddy fields next to them. As color information is used to detect Palmyra, so identical color of some paddy fields and Palmyra results in false detections at some places as shown in Fig. 4.3. However, this issue is resolved using texture analysis. Paddy fields are plain in texture compared to Palmyra trees, so

entropy is used here. Statistical measure of randomness in an image is known as Entropy that depicts the texture of the input image. Entropy is defined as

$$entropy = -\sum_i x_i log_2 x_i \quad (6)$$

Entropy value of paddy fields is found to be less compared to Palmyra, hence they are distinguished. Fig. 4.4 illustrates different texture of Palmyra and paddy fields, found using entropy.

Figure 4.3. False detections of paddy fields as Palmyra

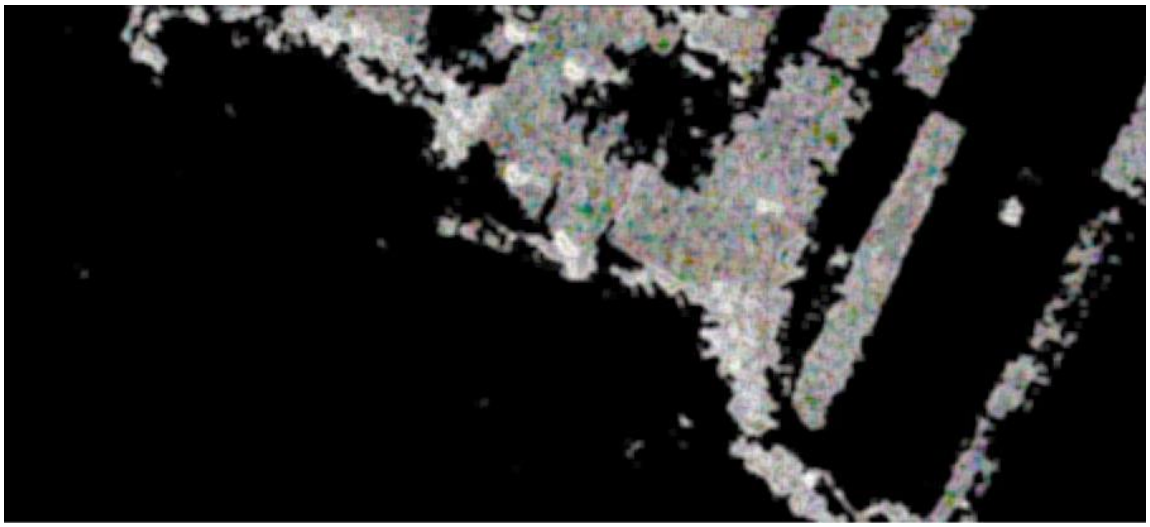

Figure 4.4. Different texture of Palmyra and paddy fields

4.2.Techniques used in QuickBird Images

4.2.1. Pan sharpening

QuickBird images of the area have different resolutions for panchromatic (0.6 m) and multispectral (2.4 m) data as shown in Fig. 4.5. Panchromatic sharpening is a radiometric transformation used to fuse a higher-resolution panchromatic image with a lower-resolution multispectral to get new raster data with high resolution spectral information. Spatial resolution of the multispectral bands is increased using panchromatic sharpening.

Many pan-sharpening algorithms exist for example Intensity-Hue-Saturation (IHS) transformation, Principal Component Substitution (PCS), the Gram-Schmidt (GS) spectral sharpening, the Brovey method and intensity modulation (IM). They differ in the extent to which they maximize the sharpness, and minimize the spectral distortion of the pan-sharpened raster image.

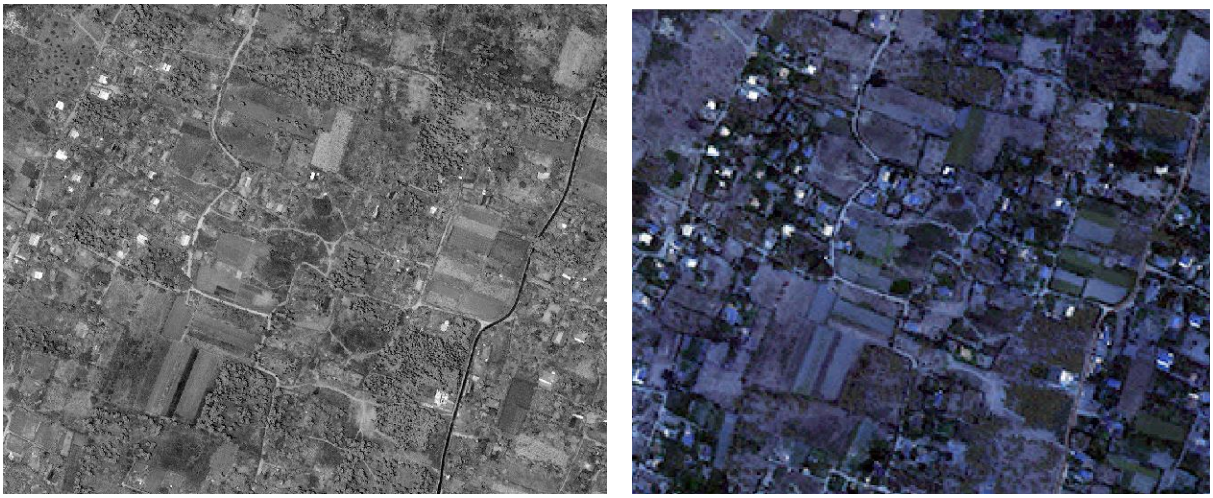

Figure 4.5. Spatial resolution of Panchromatic (0.6 m) and Multispectral (2.4 m)

Here, the Gram-Schmidt spectral sharpening method is used for pan sharpening, which is available in ArcGIS, ENVI and other software packages. The details for this method are described in [55] In first step, a simulated low resolution panchromatic (Pan_{sim}) band is created by computing a weighted average of the multispectral (*MS*) bands, as follows:

$$Pan_{sim} = \sum_{j=1}^{n} w_j MS_j \quad (7)$$

The algorithms take in non-orthogonal vectors, and then make all bands orthogonal by rotating them using the Gram-Schmidt vector orthogonalization. Iteratively, it computes the angle between Blue band and the Pan band then rotates the Blue band to make it orthogonal to the Pan band. Next, it computes the angles between the Red band and the Pan band and rotated Blue band and then make the Blue band orthogonal by rotation, and so on. This way all multispectral bands are decorrelated. The next step is to replace the low resolution simulated panchromatic band by the gain and bias adjusted high resolution panchromatic band. The weights (w_j) used for red, green, blue and NIR are 0.85, 0.7, 0.35, and 1.0 respectively. The last step is to reverse the forward Gram Schmidt transform using the same transform coefficients, but on the high-resolution bands. The result of this backward Gram- Schmidt transform is the pan-sharpened image in high resolution. Pan-sharpened image is shown in Fig. 4.6, objects such as trees, houses and street are now distinct in this high-resolution image.

Figure 4.6. Pan-sharpened Image

4.2.2. Multi-resolution Segmentation

For segmentation of Palmyra tree objects, based on its spectral properties, multiresolution segmentation is used here. Among other region merging techniques, this one is widely used in remote sensing images. The smaller objects are formed with identical pixels, which are then combined to form large objects. The objects are merged based on similarity of feature values of adjacent image objects. The degree of fitting between the objects is calculated, and its called scale parameter. The procedure stops once there are no possible merges. The two main components of multiresolution segmentation are

- Decision heuristics to find the image objects for a merge.
- Homogeneity criteria of image objects to compute the degree of fitting.

4.2.2.1. Decision Heuristics:

For a merge, a method is required to determine the image objects. Different heuristics can be applied to find an adjacent object B for the merge with an arbitrary object A. For example, merges can start from any object and its neighbor, or merge with neighbor with which similarity is maximum.

4.2.2.2. Homogeneity criteria

Difference between adjacent image objects can be one of criteria for finding the degree of fitting. For a given feature space *f*, two image objects are alike which are near to each other in this feature space. For a d-dimensional feature space the degree of fitting *h* can be:

$$h = \sqrt{\sum_{d} (f_{1d} - f_{2d})^2} \tag{8}$$

The relevant object features can be average spectral values or texture value of features and also the variance of spectral values. The distances can be standardized by the standard deviation of all sections of the feature in each dimension:

$$h = \sqrt{\sum_{d} (\frac{f_{1d} - f_{2d}}{\sigma_{fd}})^2} \tag{9}$$

4.2.2.3. Scale parameter

The primary factor in multiresolution is the scale parameter, it controls the size of the image objects. Objects are merged together until threshold reaches the scale parameter value. The scale parameter is weighted with parameters like shape and compactness to minimize fractal borders of the objects. The larger size of the objects due to a large-scale value, takes less time, but the resolution for classification is decreased. The scale size should be such that each image object or segment defines a distinct object of interest. For complex shapes, small scale values can be used but it will take more time and it will be difficult to select relevant features for an interested object. Fig. 4.7 shows the increase in object size with an increase of scale.

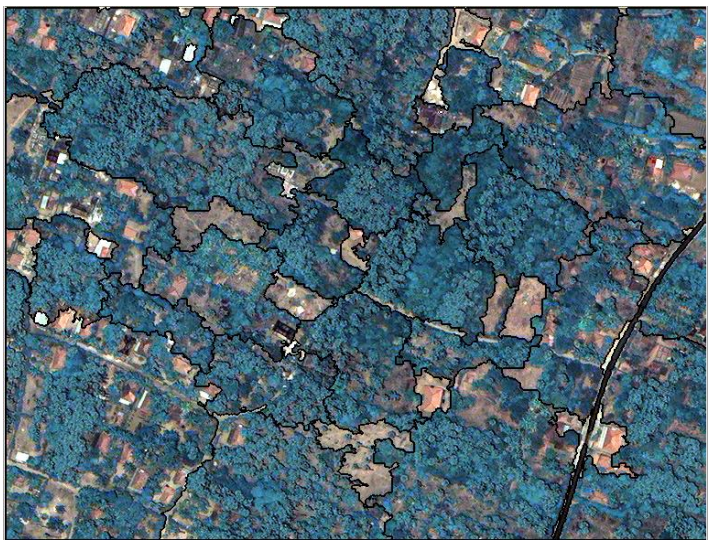

a. Scale size = 100

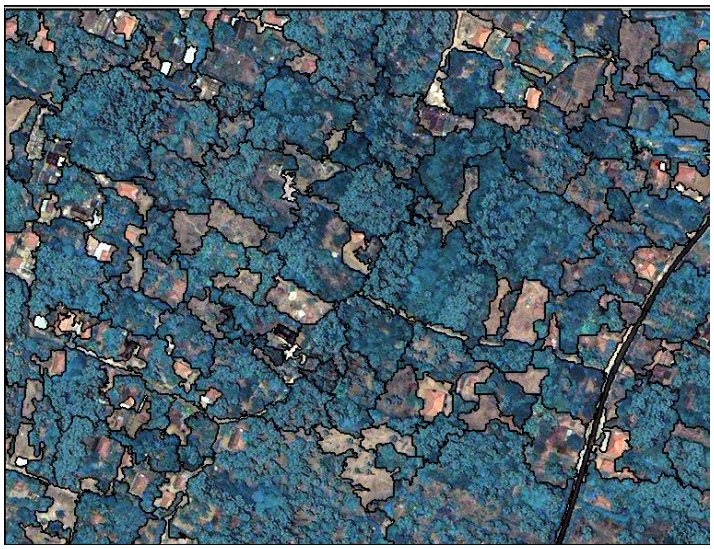

b. Scale size = 75

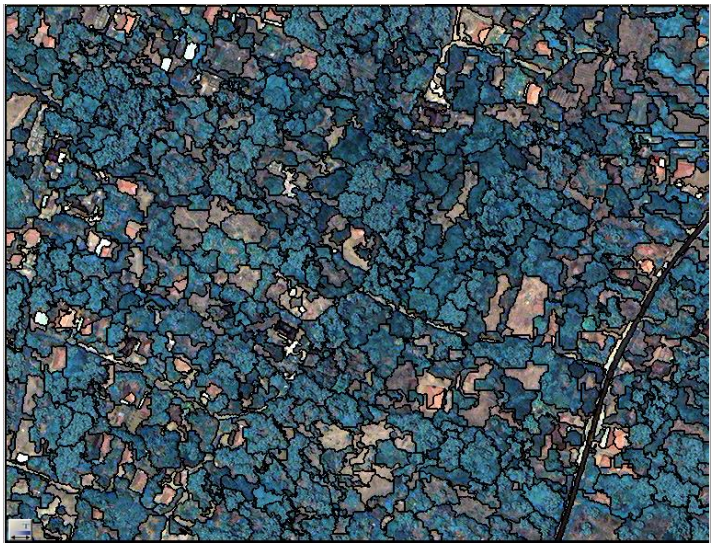

c. Scale size = 50

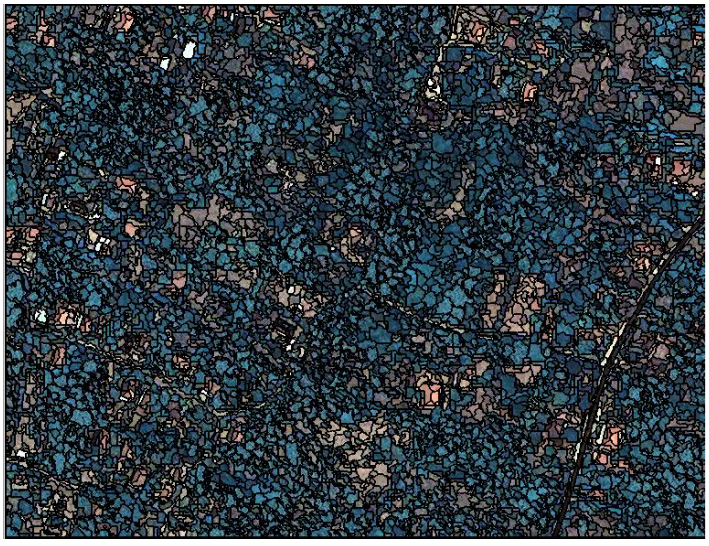

d. Scale size = 25

Figure 4.7. Effect of scale parameter on size of object segments

4.2.3. Image Object features

In supervised classification, the network is trained using some relevant and distinct features of data. To classify image objects as 'Palmyra' and 'non-Palmyra', mean layer values and GLCM feature values are used.

4.2.3.1. Mean layer values

Healthy vegetation has its spectral signature in range of Red and Near Infrared spectral bands. From the QuickBird image, it can be seen that Palmyra trees have a distinct color compared to other vegetation in the area. So, the first two object features used for classification are mean layer values of red and near infrared bands. As shown in Fig. 4.8, for Palmyra trees, mean red value is around 280 while near infrared value is in range of 800-980.

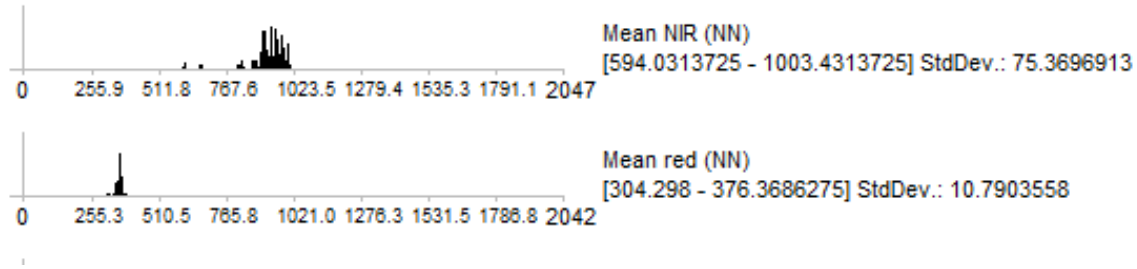

Figure 4.8. Feature value of red and NIR band for Palmyra

4.2.3.2. GLCM features

The GLCM, also known as the gray-level spatial dependence matrix is a numerical method of observing texture that considers the spatial relationship of pixels. In GLCM function relationship between pairs of pixels is calculated. A GLCM is created by finding occurrence of specific values and spatial relationship of pair of pixels, and then extracting statistical measures from this matrix.

The GLCM is calculated on the basis that how often a pixel with gray-level (grayscale intensity or level or tone) value *i*, occurs either horizontally, vertically, or diagonally to adjacent pixels with the value *j*. Two GLCM features used here to characterize Palmyra are following:

- **GLCM Contrast:** GLCM contrast is the measure of the intensity contrast between a pixel and its neighbor over the whole image through local contrast matching in GLCM matrix. Contrast is 0 for a constant image.

$$C = \sum_{i,j} |i-j|^2 p(i,j) \tag{10}$$

- **GLCM Homogeneity:** It measures the closeness of the distribution of elements in the GLCM to the GLCM diagonal.

$$H = \sum_{i,j} \frac{p(i,j)}{1+|i-j|} \tag{11}$$

Fig. 4.9 shows distinct values of GLCM contrast and homogeneity for Palmyra trees.

Figure 4.9. GLCM contrast and Homogeneity values for Palmyra

4.2.4. Classification

The final step is to classify image objects as 'Palmyra'. Using distinct values of the Red and NIR band for Palmyra, all image objects in the image are classified as 'Palmyra' and 'non-Palmyra'. In some areas lone Palmyra trees were missed and in others the coconut trees were detected as the Palmyra due to their somewhat same spectral reflectance.

4.2.4.1. Nearest Neighbor Classification

To remove false positives from the detections, the class 'Palmyra' was further refined using nearest neighbor classification. The class 'Palmyra' was divided into 'actual Palmyra' and 'other trees', using the texture features of the Palmyra.

The *k*-nearest neighbors algorithm (*k*-NN) is a simple machine learning algorithm used for classification and regression. When *k* is equal to 1, then a metric is defined to find nearest neighbor. This metric can be Euclidean, Mahalanobis or Hamming distance or simply the difference between feature values.

In the training stage, feature vectors are stored and labels are assigned to training samples. Then in the classification stage, *k* is defined. It is usually an odd number in case of binary classes. Then closet *k* neighbors based on metrics are found and that class is assigned which is most frequent among those neighbors.

When distribution of classes is skewed, the "majority voting" classification gives false results. That is, samples of a more repeated class are likely to dominate the estimate of the new sample, because they tend to be mutual among the *k* nearest neighbors due to their large quantity.

A special case of *k*-NN is where the class is estimated to be the class of the closest training sample. So when $k = 1$, it is called nearest neighbor algorithm. The accuracy of the *k*-NN algorithm can be despoiled by the presence of irrelevant or noisy features.

Here, the nearest neighbor method is used with $k = 1$, with GLCM contrast and homogeneity as class features. The number of samples used for training must be more than ten. The two classes are ‘actual Palmyra’ and ‘other trees’. Class is assigned to the neighbor which is closest to the sample feature value. It results in removal of almost all coconut trees, and thus reduced number of false positives in detection results.

5.RESULTS AND DISCUSSION

5.1. Detections on Google Earth images

The method used shows promising results in detecting Palmyra trees in Google Earth images with a high precision.

5.1.1. Foliage and Edge detection

Foliage detection using hysteresis thresholding is shown in Fig 5.1. Detection is not accurate due to general issues of thresholding and shows over-detection of foliage. Selecting thresholds that do not miss important information and add less noise needs experimentations.

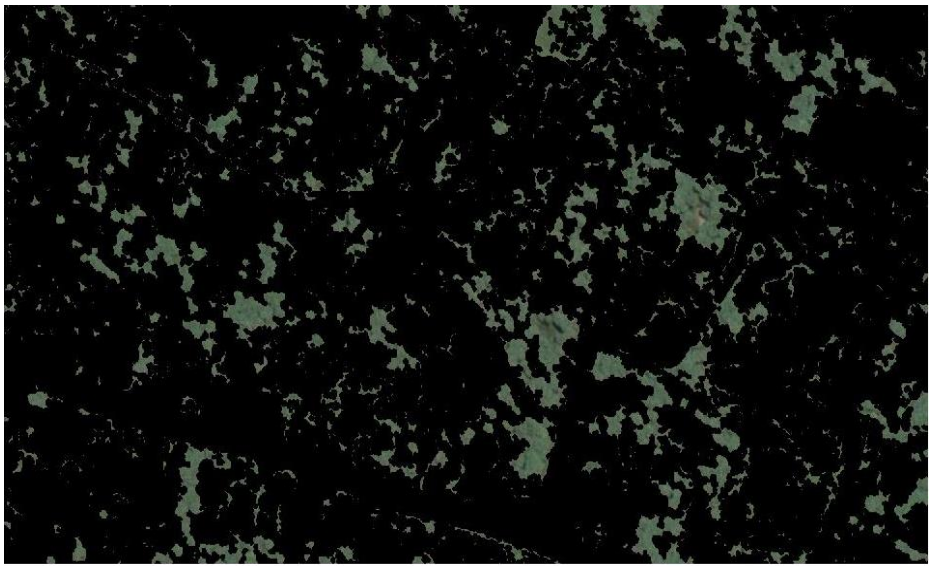

Figure 5.1. Foliage detection using hysteresis thresholding

Fig. 5.2 shows final tree edges after applying a binary threshold of 0.35 to PST output image. Edges are plotted in red for visibility.

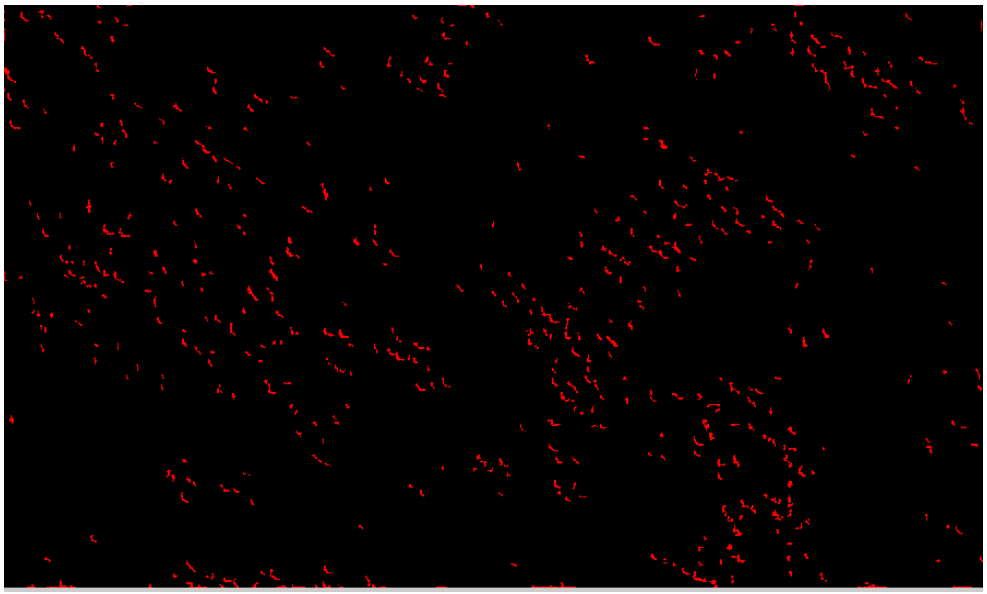

Figure 5.2. Edges after thresholding PST output

5.1.2. Overall detection

Final detection of trees after applying trapezoid mask and removing false detections is shown in Fig 5.3. Figure 5.4 shows detected blobs overlaid on the original image.

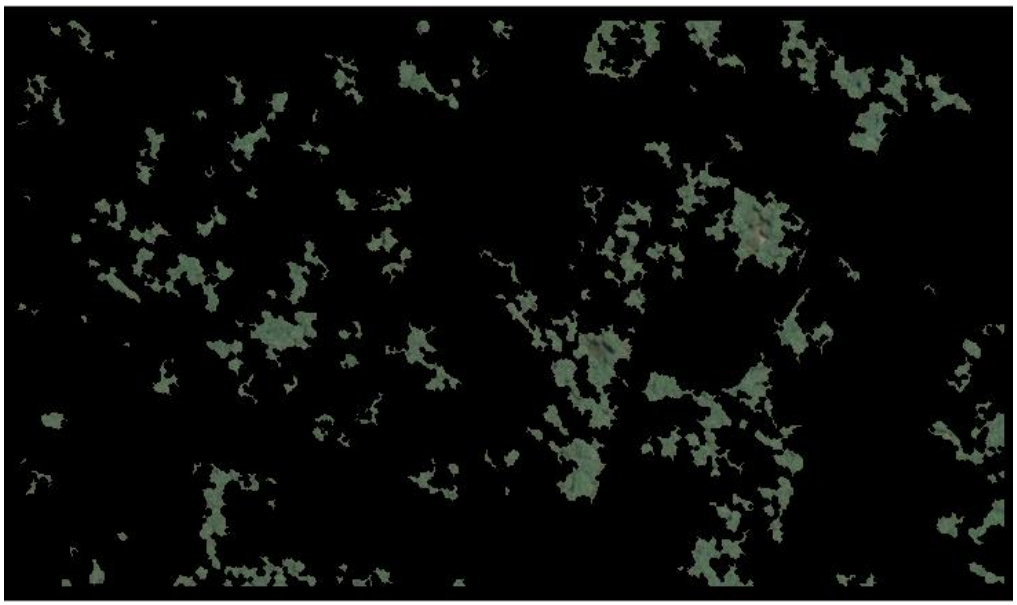

Figure 5.3. Final detection of Palmyra trees

Figure 5.4. Detected tree blobs on original image

5.1.3. Tree Counting

Edges alone are a good characteristic for detecting and counting lone trees, as seen in Fig. 4.2 (b) but for a group of trees another approach is used. Large blobs are enclosed in a rectangle and hexagonal grid of estimated tree crown radius size is fitted inside the rectangle. Number of trees in groves are found out by detecting the number of hexagon centers lying within the blob. A circular grid can also be used for estimation of trees in groves. Figure 5.5 shows hexagonal grid on a small area of groves.

Number of true positives found out to be 996, false positives and negatives are 79 and 135 respectively. The precision and recall are found to be 92.6% and 88% respectively.

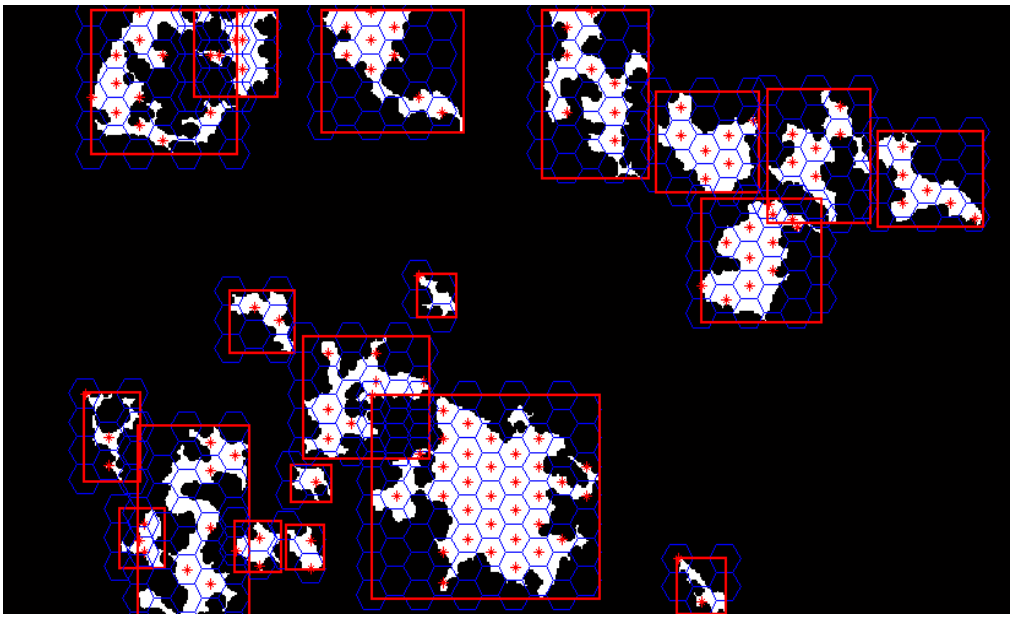

Figure 5.5. Hexagon grid for tree counting

5.2. Detections on QuickBird Images

Fig. 5.6 shows an original image of an urban area where houses, roads, land, Palmyra, coconut trees and other vegetation are shown.

Figure 5.6. Original QuickBird Image displayed in RGB

5.2.1. Segmentation

Fig. 5.7 shows segmentation results when multi-resolution segmentation is applied with a scale of 40. Image objects of Palmyra trees are well differentiable among other objects. To account for lone trees scale size is chosen to be small so that they are also contained in a single image object.

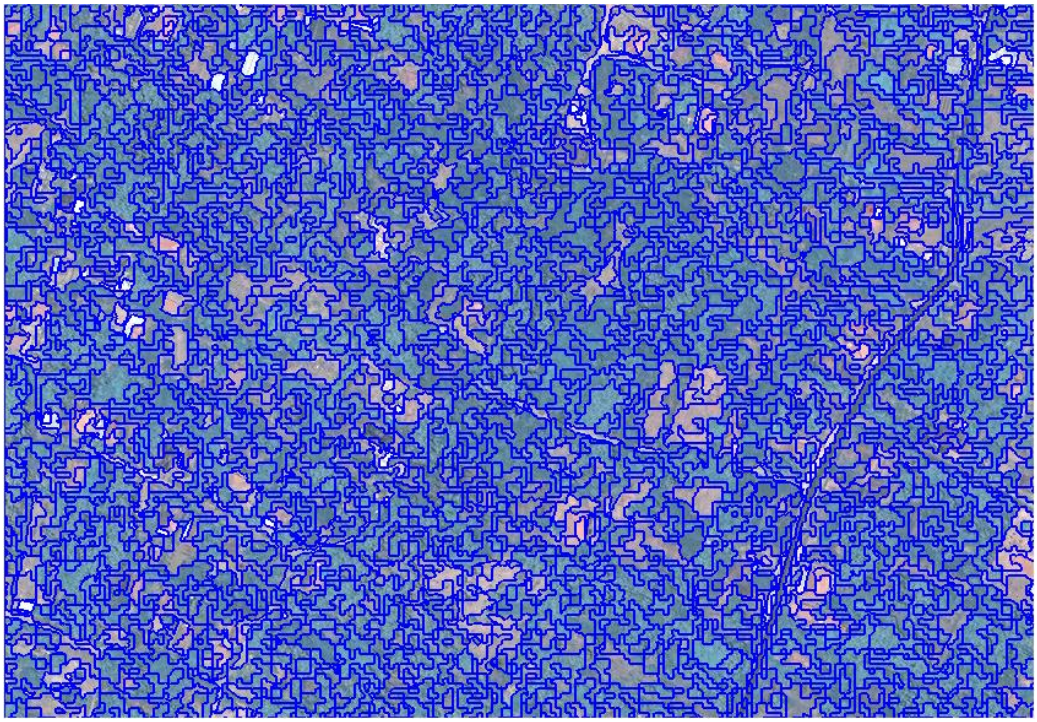

Figure 5.7. Multi-resolution segmentation

5.2.2. Classification

Fig 5.8 shows results of nearest neighbor classification on segmented image with four object features i.e. red and NIR layer values and GLCM contrast and homogeneity values. Palmyra tree foliage are shown in green color in Fig 5.9.

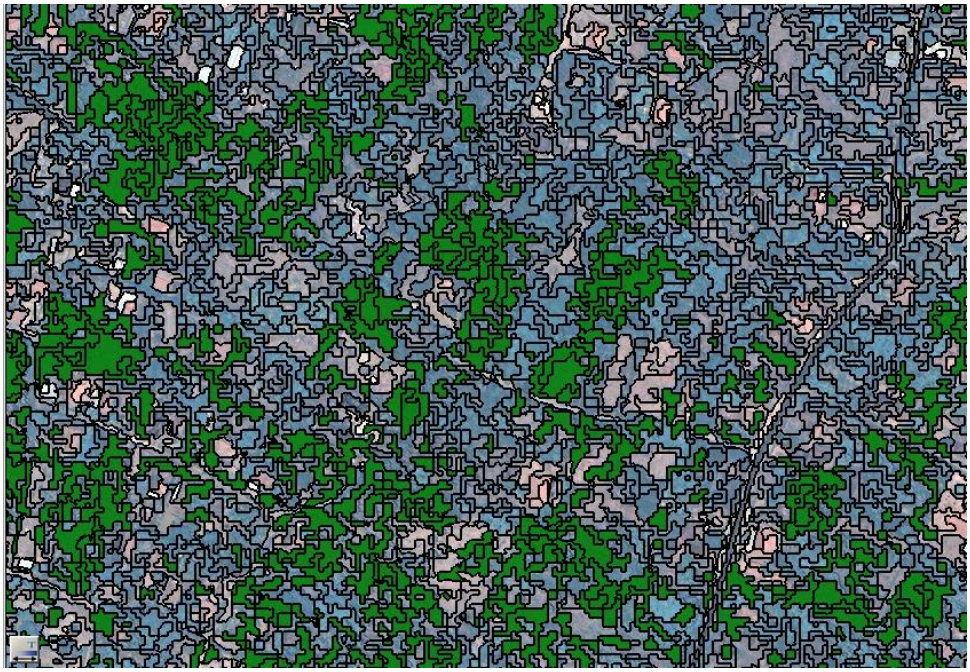

Figure 5.8. Classification results

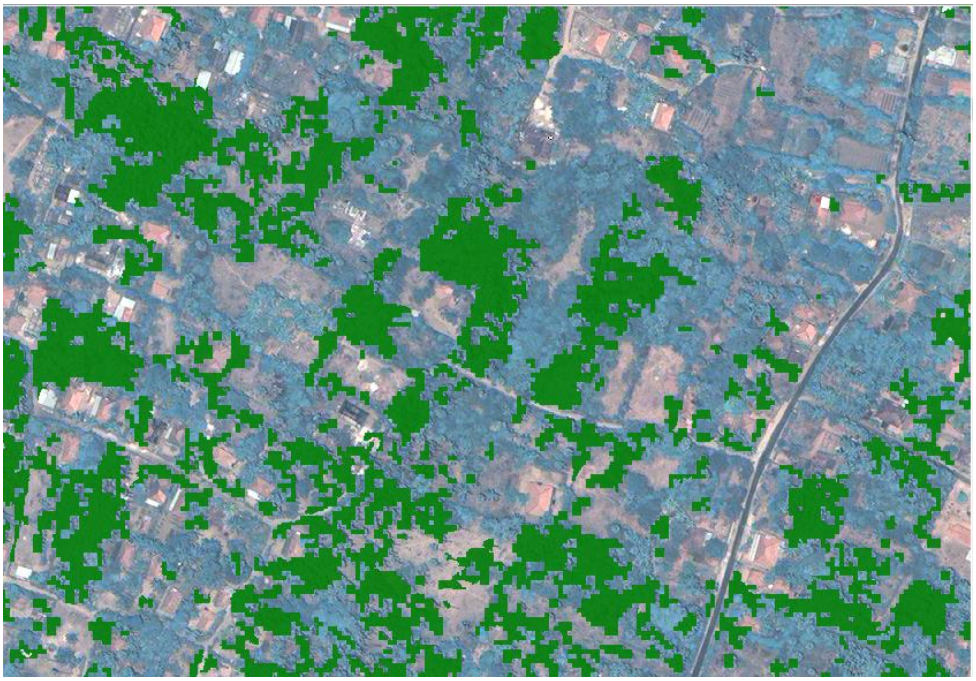

Figure 5.9. Palmyra highlighted in green

5.2.3. Overall Detection

Final detected boundaries of Palmyra trees overlaid on the original image are shown in Fig 5.10.

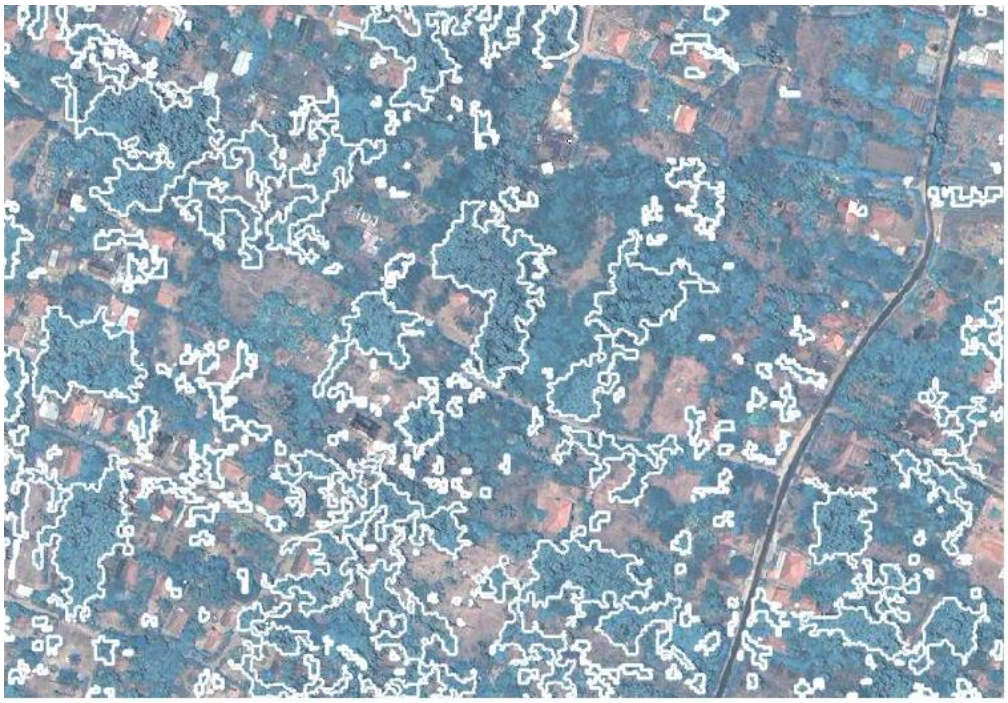

Figure 5.10. Detected tree blobs on original image

5.2.4. Tree counting

Here again, tree counting is done using hexagons, blobs are enclosed in a rectangle and hexagonal grid of estimated tree crown radius size is fitted inside the rectangle. Number of trees in groves are found out by detecting the number of hexagon centers lying within the blob. Figure 5.11 shows hexagonal grid on a small area of groves.

Number of true positives found out to be 452, false positives and negatives are 38 and 21 respectively. The precision and recall are found to be 92% and 95.5% respectively.

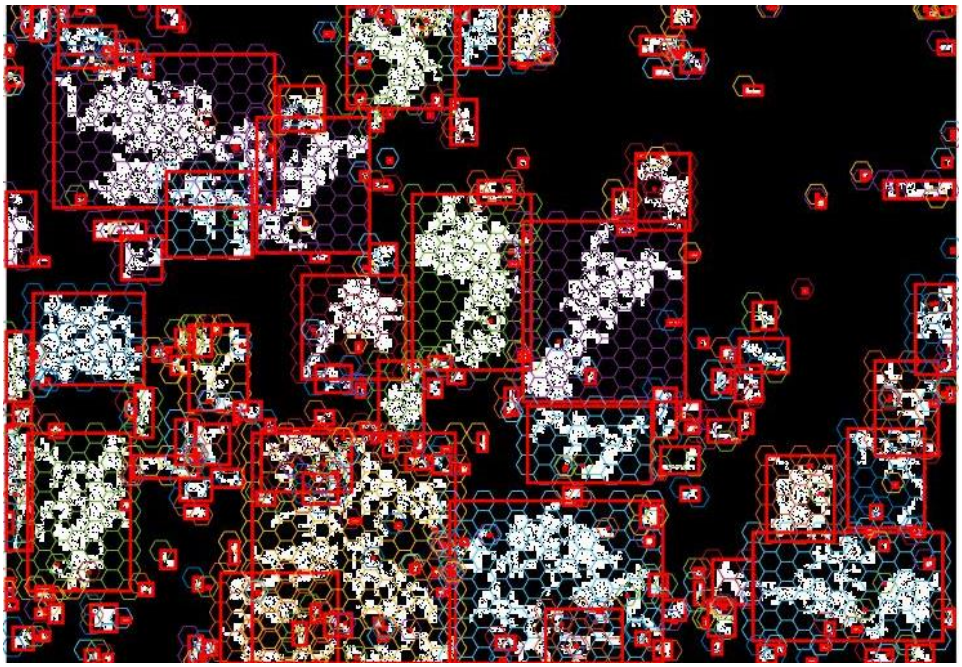

Figure 5.11. Hexagonal Grid for Tree Counting

6.CONCLUSION AND FUTURE WORK

6.1. Conclusions

This research presents the first effort in the palmyra detection or counting, which is an important task in forest density mapping. In this research, a novel method for palmyra detection is presented using Google Earth and high resolution QuickBird images. The spectral properties of palmyra along with their significant shadow is used in detection in Google Earth images. The Phase Stretch Transform is used for detection of shadow of these trees. The blob analysis ensures that all false positives are removed from detection results.

Number of techniques are applied on QuickBird images, firstly resolution of multispectral image is increased using Gram- Schmidt spectral sharpening algorithm. Then, object based image analysis is applied. Multiresolution segmentation is used in conjunction with Nearest Neighbor Classification of Palmyra trees.

Both visual interpretation and qualitative results shows promising detection results on both datasets. The performance of the algorithm is evaluated via the precision and recall values. The precision and recall are found to be 92.6% and 88% respectively for Google Earth Images. The precision and recall are found to be 92% and 95.5% respectively for QuickBird Images.

Remote sensing techniques can be used for automatic detection of Palmyra trees and their census.

- For the first time, Palmyra trees are detected using remote sensing techniques.
- Google Earth images are utilized for tree type detection.
- Different techniques are used for successful detection of Palmyra on both datasets.

6.2. Future Work

Although identification of Palmyra is done to a good extent, there are difficulties in using this technique for any general Google Earth images due to contrast issues, etc. for the rest of the Jaffna region. Hence in future, it is proposed to use QuickBird in fusion with Google Earth data

to train a model to detect the trees in other areas of Jaffna. The multimodal analysis can be carried about to estimate rate of deforestation in the area. The detection can be done using shape-based descriptors or other statistical approaches. Some sophisticated methods can be used for counting of trees in groves.

7.REFERENCES

[1] V. L. Chopra and K. V. Peter, "Handbook of industrial crops", Food Products Press, 2005, pp:384-386.

[2] S. P. Lennartz, R. G. Congalton, "Classifying and Mapping Forest Cover Types Using IKONOS Imagery in the Northeastern United States". *ASPRS Annual Conference Proceedings,* 2004.

[3] B. A. Margono, S. Turubanova, I. Zhuravleva, P. Potapov, A. Tyukavina, A. Baccini, S. Goetz, M. C. Hansen, "Mapping and monitoring deforestation and forest degradation in Sumatra (Indonesia) using Landsat time series data sets from 1990 to 2010". *Environmental Research Letters,* 2012, pp: 16.

[4] F. M. Qamer, K. Shehzad, S. Abbas, M. S. R. Murthy, C. Xi, H. Gilani, B. Bajracharya, "Mapping Deforestation and Forest Degradation Patterns in Western Himalaya, Pakistan". *Remote Sensing*, 2016, Vol. 8, pp: 385-403.

[5] A. F. de Resende, B. W. Nelson, B. M. Flores, D. R. de Almeida, "Fire Damage in Seasonally Flooded and Upland Forests of the Central Amazon". *The Association for Tropical Biology and Conservation*, 2014, vol. 46, pp: 643–646.

[6] R. K. Jaiswal, S. Mukherjee, K. D. Raju, R. Saxena, "Forest fire risk zone mapping from satellite imagery and GIS". *International Journal of Applied Earth Observation and Geoinformation*, 2002, vol. 4, pp: 1–10.

[7] X. Dong, G. Shao, D. Limin, H. Zhanqing, T. Lei, W. Hui, "Mapping forest fire risk zones with spatial data and principal component analysis". *Science in China*: *Series E Technological Sciences,* 2006, Vol. 49, pp: 140—149.

[8] C. Mering, J. Baro and E. Upegui, "Retrieving urban areas on Google Earth images: application to towns of West Africa", *International Journal of Remote Sensing*, 2010, Vol. 31, No. 22, pp: 5867–5877

[9] J. Guo, L. Liang and P. Gong, "Removing shadows from Google Earth images", *International Journal of Remote Sensing*, 2010, Vol. 31, No. 6, PP: 1379–1389

[10] S. Y. Cha and C. H. Park, "The utilization of Google Earth images as reference data for multispectral land cover classification with MODIS data of North Korea", *Korean Journal of Remote Sensing*, 2007, Vol. 23, No. 25, pp: 483-491

[11] D. Kaimarisa, O. Georgoulab, P. Patiasb, and E. Stylianidis, "Comparative analysis on the archaeological content of imagery from Google Earth", *Journal of Cultural Heritage*, 2011, Vol. 12, pp: 263–269

[12] J. R. Taylor and S. T. Lovell, "Mapping public and private spaces of urban agriculture in Chicago through the analysis of high-resolution aerial images in Google Earth", *Landscape and Urban Planning*, 2012, Vol. 108, Issue 1, pp: 57–70

[13] P. Ploton, R. L. P. Lissier, and C. Proisy, "The´ O Flavenot, Nicolas Barbier, S. N. Rai, Pierre Couteron, 2012. Assessing aboveground tropical forest biomass using Google Earth", *Ecological Applications*, 2012, Vol. 22, pp: 993–1003

[14] D. J. Nowak and E. J. Greenfield, "Tree and impervious cover change in U.S. cities", *Urban Forestry & Urban Greening*, 2012, Vol. 11, pp: 21– 30.

[15] Q. Hu, W. Wu, T. Xia, Q. Yu, P. Yang, Z. Li and Q. Song, "Exploring the Use of Google Earth Imagery and Object-Based Methods in Land Use/Cover Mapping", *Remote Sensing*, 2013, Vol. 5, pp: 6026-6042.

[16] F. A. Gougeon and D. G. Leckie, "The individual tree crown approach applied to IKONOS images of a coniferous plantation area". *Photogrammetric Engineering and Remote Sensing*, 2005, Vol. 72, pp: 1287-1297.

[17] H. Z. M. Shafri, N. Hamdan, and, M. I. Saripan , "Semi-automatic detection and counting of oil palm trees from high spatial resolution airborne imagery. International Journal of Remote Sensing",2011, Vol. 32, pp: 2095–2115.

[18] M. T. Gebreslasie, F. B. Ahmed, J. A. N. Van Aardt and, F Blakeway, "Individual tree detection based on variable and fixed window size local maxima filtering applied to IKONOS imagery for even-aged Eucalyptus plantation forests". *International Journal of Remote Sensing*, 2011, Vol. 32, pp: 4141–4154.

[19] P. Srestasathiern and P. Rakwatin, "Oil Palm Tree Detection with High Resolution Multi-Spectral Satellite Imagery", *Remote Sens*ing, 2014, Vol. 6, pp: 9749-9774.

[20] M. dos Santos, D. Mitja, E. Delaître, L. Demagistri, I.S. Miranda, T. Libourel, and M. Petit, "Estimating babassu palm density using automatic palm tree detection with very high spatial resolution satellite images", *Journal of Environmental Management*, 2017, Vol. 193, pp: 40-51

[21] Puissant, Corres, J. Hirsch, C. Weber, "The utility of texture analysis to improve per-pixel classification for high to very high spatial resolution imagery". *International Journal of Remote Sensing*, 2005, Vol. 26, pp: 733-745.

[22] F. Pacifici, M. Chini, W. J. Emery, "A Neural Network Approach using Multi-Scale Textural Metrics from Very High-resolution Panchromatic Imagery for Urban Landuse Classification". *Remote Sensing of Environment*, 2009, vol. 113, pp: 1276-1292.

[23] D. S. Culvenor, "TIDA: An algorithm for the delineation of tree crowns in high spatial resolution remotely sensed imagery" *Comput. Geosci.* 2002, Vol. 28, pp: 33–44.

[24] J. Yang, Y. He, J. Casperson, "A Multi-Band Watershed Segmentation Method for Individual Tree Crown Delineation from High Resolution Multispectral Aerial Image". *IEEE International Geoscience and Remote Sensing Symposium*, 2014.

[25] T. Hofmann, J. Puzicha, J. Buhmann, "Unsupervised texture segmentation in a deterministic annealing framework". *IEEE Transactions on Pattern Analysis and Machine Intelligence*, 1998, Vol. 20, pp: 803-818.

[26] C. S. Won, H. Derin, "Unsupervised segmentation of noisy and textured images using Markov random fields". *CVGIP: Graphical Models and Image Processing*, 1992, Vol. 54, pp: 308-328.

[27] D. Panjwani, G. Healey, "Markov random field models for unsupervised segmentation of textured color images". *IEEE Transactions on Pattern Analysis and Machine Intelligence*, 1995, Vol. 17, pp: 939-954.

[28] R. Haralick, K. Shanmugan, I. Dinstein, "Textural features for image classification". *IEEE Transactions on Systems, Man and Cybernetics*, 1973. Vol. 3, pp: 610-621.

[29] E. Salari, Z. Ling, "Texture Segmentation using hierarchical Wavelet Decomposition". *Pattern Recognition*, 1995, Vol.28, pp: 1819-1824

[30] P. Bunting, R. Lucas, "The delineation of tree crowns in Australian mixed species forests using hyperspectral Compact Airborne Spectrographic Imager (CASI) data". *Remote Sensing of Environment*, 2006, vol. 101, pp: 230-248.

[31] T. Kavzoglu., P.M. Mather, "The Use of Backpropagating Artificial Neural Networks in Land Cover Classification". *International Journal of Remote Sensing*, 2003, Vol. 24, pp: 4907-4938.

[32] H. Jiang, D. Zhao, Y. Cai, S. An, "A Method for Application of Classification Tree Models to Map Aquatic Vegetation using Remotely Sensed Images from Different Sensors and Dates". 2012, Vol. 12, pp: 12437-12454.

[33] P.O. Gislason, J. A. Benediktsson, J. R. Sveinsson, "Random Forests for Land Cover Classification". *Pattern Recognition Letters*, 2006, Vol. 27, pp: 294-300.

[34] Puissanta, S. Rougiera, A. Stumpf, "Object-oriented mapping of urban trees using Random Forest classifiers". *International Journal of Applied Earth Observation and Geoinformation*, 2013, vol. 26, pp: 235–245.

[35] J. S. H. Lee, S. Wich, A. Widayati, L. P. Koh, "Detecting industrial oil palm plantations on Landsat images with Google Earth Engine". *Remote Sensing Applications: Society and Environment*, 2016, vol. 4, pp: 219–224.

[36] Shalaby, R. Tateishi, "Remote Sensing and GIS for Mapping and Monitoring Land Cover and Land-use Changes in the Northwestern Coastal Zone of Egypt". *Applied Geography*, 2007, vol. 27, pp: 28-41.

[37] S. R. Garrity, C. D. Allen, S. P. Brumby, C. Gangodagamage, N. G. McDowell, D. M. Cai, "Quantifying tree mortality in a mixed species woodland using multitemporal high spatial resolution satellite imagery". *Remote Sensing of Environment*, 2013, Vol. 129, pp: 54–65.

[38] M. H. Tseng, S. J. Chen, G. H. Hwang, M. Y. Shen, "A Genetic Algorithm Rule-based Approach for Land-cover Classification". *ISPRS Journal of Photogrammetry and Remote Sensing*, 2008, vol. 63, pp: 202-212.

[39] C. Lardeux, P. L. Frison, C. Tison, J. C. Souyris, B. Stoll, B. Fruneau, J. P. Rudant, "Support vector machine for multifrequency SAR polarimetric data classification". *IEEE Transactions on Geoscience and Remote Sensing*, 2009, vol. 47, pp: 4143–4152.

[40] M. Dalponte, L. Bruzzone, D. Gianelle, "Fusion of hyperspectral and LIDAR remote sensing data for classification of complex forest areas". *IEEE Transactions on Geoscience and Remote Sensing*, 2008, vol. 46, pp: 1416–1427.

[41] Huang, H., Gong, P., Clinton, N., Hui, F., 2008b. Reduction of atmospheric and topographic effect on Landsat TM data for forest classification. International Journal of Remote Sensing 29 (19), 5623–5642.

[42] Y. Xie, Z. Sha, M. Yu, "Remote sensing imagery in vegetation mapping: a review". *Journal of Plant Ecology*, 2008, vol. 1, pp: 9-23.

[43] F. Morsdorf, E. Meiera, B. Kötza, K. I. Ittena, M. Dobbertinc, B. Allgöwer., "LIDAR-based geometric reconstruction of boreal type forest stands at single tree level for forest and wildland fire management". *Remote Sensing of Environment*, 2004, Vol. 92, pp: 353–362.

[44] E. Blanzieri, F. Melgani, "Nearest neighbor classification of remote sensing images with the maximal margin principle". *IEEE Transactions on Geoscience and Remote Sensing*, 2008, vol. 46, pp: 1804-1811.

[45] Gonçalves M.L., Netto M.L.A., Costa J.A.F., Zullo Júnior J. (2008) - An Unsupervised Method of Classifying Remotely Sensed Images using Kohonen Self

organizing Maps and Agglomerative Hierarchical Clustering Methods. International Journal of Remote Sensing, 29: 3171-3207.

[46] Q. Yu, P. Gong, N. Clinton, G. Biging, M. Kelly, D. Schirokauer, "Object-based Detailed Vegetation Classification with Airborne High Spatial Resolution Remote Sensing Imagery". *Photogrammetric Engineering & Remote Sensing*, 2006, Vol. 72, pp: 799–811.

[47] Z. Xie, C. Roberts, B. Johnson, "Object-based target search using remotely sensed data: A case study in detecting invasive exotic Australian Pine in south Florida". *ISPRS Journal of Photogrammetry & Remote Sensing*, 2008

[48] J. P. Ardila, W. Bijker, V. A. Tolpekin, A. Stein, "Context-sensitive extraction of tree crown objects in urban areas using VHR satellite images". *International Journal of Applied Earth Observation and Geoinformation*, 2012, Vol. 15, pp: 57–69

[49] M. S. Tehrany, B. Pradhan, M. N. Jebuv, "A comparative assessment between object and pixel-based classification approaches for land use/land cover mapping using SPOT 5 imagery". Geocarto International, 2014, vol. 29, pp: 351-369.

[50] Candere

[51] G. Mallinis, N. Koutsias, M. T. Strati, M. Karteris, "Object-based classification using Quickbird imagery for delineating forest vegetation polygons in a Mediterranean test site". *ISPRS Journal of Photogrammetry and Remote Sensing*, 2008, Vol. 63, pp: 237-250.

[52] F. M. B. Van Coillie, L. P. C. Verbeke, R. R. D. Wulf, "Feature selection by genetic algorithms in object-based classification of IKONOS imagery for forest mapping in Flanders, Belgium". *Remote Sensing of Environment*, 2007, Vol. 110, pp: 467-487.

[53] D. L. Olson and D. Delen, "Advanced Data Mining Techniques", Springer, 1st edition, pp: 138.

[54] M. H. Asghari and B. Jalali, "Edge Detection in Digital Images Using Dispersive Phase Stretch Transform," International Journal of Biomedical Imaging, Volume 2015, Article ID 687819, 6 pages

[55] T. Maurer, "How to Pan-Sharpen Images Using the Gram-Schmidt Pan-Sharpen Method – A Recipe". *International Archives of the Photogrammetry, Remote Sensing and Spatial Information Sciences*, 2013, Vol. XL-1/W1.

[56] M. Baatz, A. Schäpe, "Multiresolution segmentation: an optimization approach for high quality multi-scale image segmentation". *XII Angewandte Geographische Informationsverarbeitung*, Wichmann-Verlag, Heidelberg, 2000.